Chapter 9
Green Synthesis of Iron Oxide Nanoparticles: Cutting Edge Technology and Multifaceted Applications

Rakesh K. Bachheti, Rocktotpal Konwarh, Vartika Gupta, Azamal Husen, and Archana Joshi

9.1 Introduction

Nanotechnology represents a realm of cross-fertilized ideas and concepts. It encompasses a myriad of innovative tools and approaches that have seeded a plethora of products for a wide gamut of applications (Konwarh et al. 2009, 2012; Husen and Siddiqi 2014; Kumar et al. 2017; Siddiqi et al. 2018a, b). Be it waste-water treatment, efficient ferrying and targeted delivery of bio-cargoes including the therapeutic/bioactive molecules, tissue engineering or optoelectronics, nanotechnology has etched an indelible mark on the scientific canvas (Barua et al. 2013; Pramanik et al. 2013; Mobasser and Firoozi 2016; Reardon et al. 2017). The number of research papers and patents on applications of nanomaterials has grown by leaps and bounds over the last few years. It may be recalled that nanoscience and nanotechnology deal with the efficient coalescing of biological, chemical and engineering approaches to control/manipulate materials within the nanoscale range (1–100 nm). The unique shape-size-surface chemistry accord of various nanomaterials has endowed them

R. K. Bachheti (✉)
Department of Industrial Chemistry, Addis Ababa Science and Technology University, Addis Ababa, Ethiopia

R. Konwarh
Department of Biotechnology, Addis Ababa Science and Technology University, Addis Ababa, Ethiopia

V. Gupta
Department of Chemistry, Graphic Era University, Dehradun, Uttarakhand, India

A. Husen
Department of Biology, College of Natural and Computational Sciences, University of Gondar, Gondar, Ethiopia

A. Joshi
Department of Environment Science, Graphic Era University, Dehradun, Uttarakhand, India

A. Husen, M. Iqbal (eds.), *Nanomaterials and Plant Potential*,
https://doi.org/10.1007/978-3-030-05569-1_9

with distinct positions in diverse domains such as biotechnology, mechanics, engineering, energy and the environment, to name a few.

Iron oxide nanoparticles (NPs) have found applications in drug delivery, immunopurification, catalysis, MRI, hyperthermia, toxic-component mitigation and so on (Siddiqi et al. 2016; Dinali et al. 2017). Biocompatibility and immune acceptance of iron oxide NPs have been discussed time and again. Use of polymeric encapsulation or coating of iron oxide NPs improves their colloidal stability in water and facilitates design of 'smart' or hybrid particles (that may be used for focused delivery of therapeutic agents) as well as greater shape-size tuning that dictates the pharmacokinetics, bio-distribution and immune clearance (Ali et al. 2016). Jun et al. (2008) discussed the various nanomagnetism scaling laws of engineered nanoparticles. The size and shape concurrences along with composition, crystallographic structure, magnetic anisotropic energy, vacancies and defects are the critical parameters for determining the magnetic properties (such as coercivity, *Hc* and susceptibility, χ) of I iron oxide NPs.

The pros and cons of the preparation protocols of iron oxide NPs like co-precipitation of iron salts, micro-emulsion approach, thermal decomposition of iron precursors, hydrothermal methods, sonochemical method, sol-gel transition, chemical vapour deposition (CVD), flow injection, electrochemical techniques under oxidizing conditions and laser-induced pyrolysis of pentacarbonyl iron vapours have been extensively reviewed (Jun et al. 2008). Some of the bottlenecks associated with these techniques are high cost, high energy consumption, applications of toxic reagents (high ecological footprint), etc. A surmounting pressure of 'going green' amongst the scientific fraternity has dictated the researchers to explore and exploit the nature's way of preparing the nanomaterials (Thakur and Karak 2015). In this context, bio-resources like fungi and bacteria have been assessed. A wealth of informative literature on phytosynthesis of different nanomaterials, including iron oxide NPs (Hassan et al. 2018; Devi et al. 2018), can be retrieved from literature databases of SCOPUS and Web of Science, etc. (Fig. 9.1).

Abundance of various reducing and capping agents in plant extracts has been crucial in the preparation of various well-stabilized nanomaterials (Siddiqi et al. 2016; Husen 2017; Siddiqi and Husen 2017). The plant-mediated preparation of iron oxide NPs is also gaining pace (Table 9.1).

Use of phytochemicals as capping agents/stabilizing agents could be a promising stratagem to lessen the side effects and increase the biocompatibility of inorganic nanoparticles for biomedical applications. However, this may not be the complete story. Even such green materials need to undergo in vitro, in vivo and eco-toxicity assessments before being commercialized for practical applications. Nevertheless, easy and abundant availability, efficiency in terms of time utility and circumvention of the use of toxic reagents are few of the desired facets of this approach (Husen 2017; Siddiqi and Husen 2017).

In this backdrop, we compile in this chapter the recent research on plant-mediated preparation of iron oxide NPs, with special focus on their prospective applications.

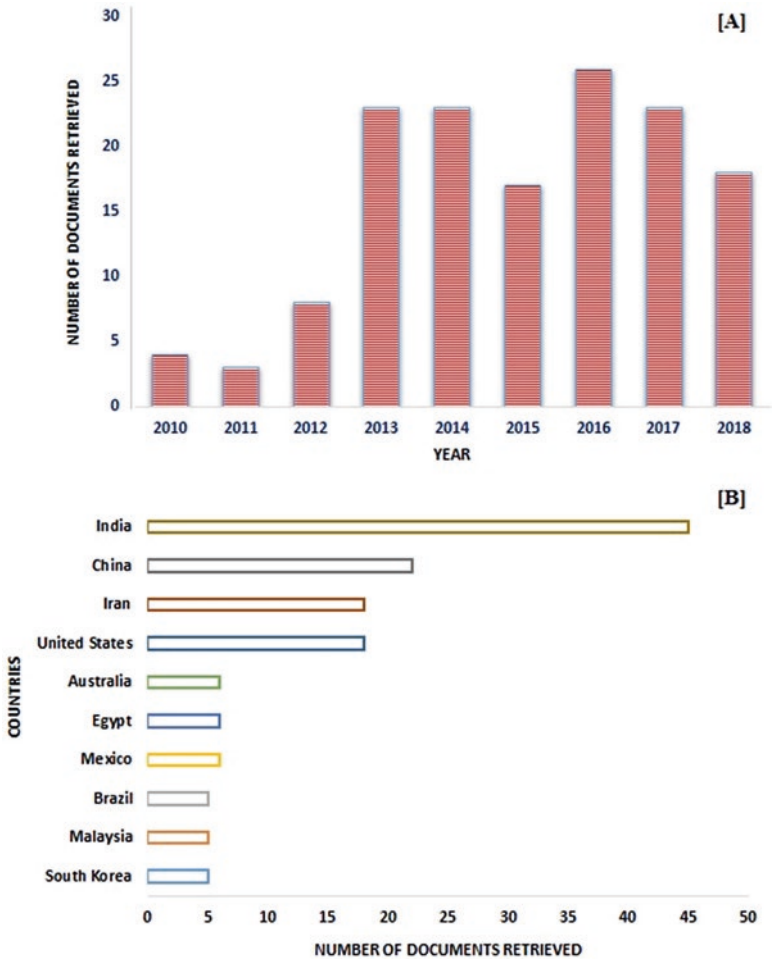

Fig. 9.1 Plots depicting the (**a**) year-wise distribution and (**b**) countries with the maximal number of scientific documents (period: 2010 to 2018) retrievable from Scopus for the search-query, 'Synthesis of iron oxide nanoparticles by plants' as on 18 June 2018

9.2 The Basics of IO-NP Phytosynthesis

9.2.1 Principle and Exemplary Illustrations

Phytosynthesis of IO-NPs represents a bottom-up strategy with oxidation/reduction being the prime reaction. The phytochemicals with antioxidant/reducing attributes mediate the reduction of various salts to their corresponding nanoparticles. A wide spectrum of plants and their active components has been explored for the synthesis of iron oxide NPs (as discussed in the subsequent sections of the chapter).

Table 9.1 Plants and their parts used for synthesis of iron oxide NPs, together with their shape and size

Plant	Plant part	Size/shape	References
Agrewia optiva and *Prunus persica*	Leaf	14–17 nm/cubic spinel structure	Mirza et al. (2018)
Aloe vera	Leaf	6–30 nm/crystalline	Phumying et al. (2013)
Cyanococcus spp.	Shoots	52.4 nm/different shape	Manquián-Cerda et al. (2017)
Camellia sinensis	Leaf	40–80 nm/spherical	Ahmmad et al. (2013)
Camellia sinensis	Leaf	5 nm ≤ crystalline	Plachtová et al. (2018)
Carica papaya	Leaf	33 nm/plate like	Latha and Gowri (2014)
Ceratonia siliqua	Leaf	4–8 nm/crystalline	Awwad and Salem (2012)
Citrus medica	Leaf	45 nm/spherical	Esam (2015)
Citrus reticulata	Peel	50 nm/spherical	Ehrampoush et al. (2015)
Curcuma longa	Plant	Spherical	Herlekar and Siddhivinayak (2015)
Cynometra ramiflora	Leaf	Crystalline	Groiss et al. (2016)
Desmodium gangeticum	Root	25–35 nm/spherical	Santoshi et al. (2015)
Excoecaria cochinchinensis	Leaves	5–20 nm/composites	Lin et al. (2018)
Hibiscus rosa-sinensis	Plant	10–15 nm/spherical	Rath et al. (2015)
Hordeum vulgare and *Rumex acetosa*	Plant	30 nm/amorphous 10–40 nm/amorphous	Makarov et al. (2014)
Juglans regia	Husk	9.7–15.4 nm/cubic shape	Izadiyan et al. (2018)
Mansoa alliacea	Leaf	30 nm/crystalline	Prasad (2016)
Medicago sativa		2–10 nm/crystalline	Herrera-Becerra et al. (2008)
Mimosa pudica	Root	67 nm/spherical and crystalline	Niraimathee et al. (2016)
Musa paradisiaca	Peel	<50 nm/polydispersed	Venkateswarlu et al. (2013)
Musa	Peel	100–200 nm/spherical	Sudha et al. (2015)
Musa acuminata and *Colocasia esculenta*	Peel/leaves	10–25 nm/cubic spinel crystal	Thakur and Karak (2014)
Ocimum sanctum	Leaf	20 nm/irregular sphere	Balamurughan et al. (2014)
Punica granatum	Peel	Amorphous	Irshad et al. (2017)
Punica granatum	Rind	Polycrystalline	Venkateswarlu et al. (2014a)
Zea mays and *Brassica rapa*	Hair of corn and cabbage	84.81 nm/crystallite sizes 48.91 nm/crystallite sizes	Patra and Baek (2017)

(continued)

Table 9.1 (continued)

Plant	Plant part	Size/shape	References
Syzygium cumini	Seed	20 nm/spherical fcc	Venkateswarlu et al. (2014b)
Terminalia chebula	Fruit pericarp	<80 nm/chain-like	Kumar et al. (2014)
Tridax procumbens	Leaf	80–100 nm/irregular spherical	Senthil and Ramesh (2012)
Vitis vinifera	Seed	30 nm/crystalline and spherical	Narayanan et al. (2012)
Vitis vinifera	Stem	<50 nm/core shell structure	Venkateswarlu et al. (2015)
Wrightia tinctoria	Plant	105–145 nm/crystalline	Sravanthi et al. (2016)

To cite for evidence, waste leaves of Oman's mango plant were used to prepare iron oxide nanorods (NRs) (Al-Ruqeishi et al. 2016). Interestingly, polyphenols like mangiferin, penta-O-galloyl-glucoside gallic acid and methyl gallate are abundant in mango (Barreto et al. 2008). These polyphenolics were envisaged to participate actively in the generation of iron oxide NRs (15 ± 2 nm in average length and 3.0 ± 0.2 nm in average diameter). As sodium hydroxide and iron sulphate interact in the aqueous medium, interaction of biomolecules of the extract of the green leaves hastens the generation of FeOOH, which dissociates yielding Fe_2O_3 nuclei. One D iron oxide NRs (the shape and size being influenced by the reaction time and temperature) are gradually built up at various places within the solution. With passage of time, Fe_2O_3 dissociates into its γ and α types. Under appropriate parameters of solution concentration, temperature and sonication, the incessant enlargement of the Fe_2O_3 nuclei leads to the attainment of the final shape of nanorod. A pivotal influence of the biomolecules of the mango leaves extract has been proposed in dictating the shape of the nanorods. Similar observations have been reported for the influence of biomolecules of plant extracts as well as bioactive molecules like enzymes on the eventual shape-size accord of various other nanomaterials as well (Konwarh et al. 2010, 2012, 2014). On the other hand, extract of *Juglans regia*'s green husk (a waste material in the walnut-production industry) is rich in phenolic compounds like vanillic acid, myricetin, coumaric acid, syringic acid, juglone and ferulic acid. The extract was efficiently exploited for the preparation of IO-NPs of high purity, with high saturation magnetization and low coercivity (Izadiyan et al. 2018). The synthesis may be summed up as underneath:

$$J.\ regia + H_2O_{(L)} + 2Fe^{+3} + Fe^{+2} \xrightarrow{\text{stirring}} \left[J.regia / 2Fe^{+3} : 1Fe^{+2} \right] \tag{9.1}$$

$$\left[J.regia / 2Fe^{+3} : 1Fe^{+2} \right] + 8OH^-_{(aq)} \rightarrow \left[J.regia / \text{iron oxide nanoparticles} \right]_{(s)} + 4H_2O_{(L)} \tag{9.2}$$

Similarly, polyphenols (in the form of tannins) present in the extract of dry fruit pericarp of *Terminalia chebula* were converted under mild acidic conditions to yield glucose, ellagic acid, gallic acid, etc. The conversion of phenolics to quinone was exploited for the reduction of iron salt to yield stabilized iron oxide nanoparticles (<80 nm) (Kumar et al. 2013).

9.2.2 Crucial Dictates of the Synthesis

A number of factors influence the phytosynthesis of nanoparticles. The various parameters, such as concentration of the salt, mixing ratio of the plant extract and metal salt, pH value, temperature, incubation time, etc., demand optimization to generate homogenous nanoparticles of a similar shape and size (Shah et al. 2015).

One of the prime determinants is the pH of the medium. Herrera-Becerra et al. (2008) reported the influence of pH on size distribution and nature of the iron oxides obtained by using alfalfa extract. Greater proportion of Fe_2O_3 particles (and a few Fe_3O_4) of smaller size was obtained at pH = 10, while pH = 3 and pH = 5 favoured the formation of FeO rhombohedral structure of larger dimensions. $Fe_{0.902}O$ cubic structures were obtained more or less in similar proportion for various pH values. The incubation time and storage conditions are another prime dictators of the quality of the phytosynthesized NPs. The effect of concentration of the reactant cannot be ruled out. Ehrampoush et al. (2015) reported that as the concentration of tangerine peel extract increased from 2% to 6%, the average size of the iron oxide NPs decreased from 200 nm to 50 nm. A point of pertinence is that the extraction protocol of the reducing/stabilizing agents, the age of the plants and plant parts (leaves, stems, flowers, fruits, etc. with varying compositional abundance of the active agents) used to prepare the extract might have a collective influence on the size, shape and distribution of iron oxide NPs. The presence of additional components in the reaction medium might exert additional influence. For instance, Gan et al. (2018) explored the use of the cationic surfactant CTAB as a stabilizing and capping agent for iron oxide NPs, prepared using eucalyptus leaf extract. The assembled surface monolayer of CTAB augmented the dispersion of the nanoparticles as well as dictated the phosphate removal efficiency via exerting influence over the micellar organization and accessibility of the lipophilic biomolecules of the leaf extract. Furthermore, the quality and quantity of synthesized NPs are affected by the procedure used for their purification.

9.2.3 Approaches for Physicochemical Characterization

A range of tools and techniques are routinely used for characterization of iron oxide NPs (Neamtu et al. 2018). Various spectroscopic and microscopic tools aid in comprehending the physicochemical properties like surface texture, size and shape,

surface functionality, aggregation state, magnetic property, thermal and dynamic properties, surface area, etc. (Can et al. 2018). Ultraviolet-(UV)-visible spectroscopy, scanning electron microscopy (SEM), transmission electron microscopy (TEM), Fourier-transform infrared spectroscopy (FTIR), X-ray diffraction (XRD), atomic force microscopy (AFM), energy-dispersive X-ray spectroscopy (EDX), dynamic light scattering (DLS), dynamic scanning calorimetry (DSC), thermal gravimetric analysis (TGA) and differential thermal analysis (DTA), dynamic mechanical analysis (DMA), Brunauer-Emmett-Teller (BET) method and vibrating sample magnetometry (VSM) are some of the tools and techniques that are used widely. A detailed description of each characterization tool is beyond the scope of this chapter. Nevertheless, as representative physicochemical approaches to understand the properties of the iron oxide NPs, results of some of the major characterization techniques are mentioned throughout the text. Khalil et al. (2017) reported the XRD spectra of *Sageretia thea* (Osbeck.) extract-based IO-NPs (annealed at 500 °C). Single pure-phase (Fe_2O_3) tetragonal maghemite was indicated by the observed Bragg peaks. Lattice constants were calculated as $<a_{exp}.> = 8.34000$ A° and $<c_{exp}.> = 25.02000$ A°. The average size of the highly crystalline IO-NPs was found to be ~29 nm as calculated using Debye-Scherrer equation. On the other hand, FTIR spectra were illustrative of absorption peak at ~500 cm^{-1} (characteristic Fe-O vibration), broad-OH stretching at ~3400 cm^{-1} (attributed to phytophenolics) and other peaks at ~1100–1200, 1600 and 2200 cm^{-1}, ascribable to the –C–O, –C=O and –CN functional groups, respectively. Raman spectra (Argon laser, $\lambda_{exc} = 514$ nm) and EDS analysis were also used. Raman shift at ~388, ~500 and ~772 cm^{-1} could be attributed, respectively, to T_{2g}, E_g and A_{1g} Raman active phonon modes specific to maghemite. EDS analysis depicted the elemental composition of the phytogenerated iron oxide NPs (peak of carbon could be ascribed to the grid support). Furthermore, various other parameters of iron oxide NPs like cytotoxicity, antioxidant capacity, anticancer activity, biodegradability, pharmacokinetics and pharmacodynamics are assessed from the biological perspective (Feng et al. 2018).

9.2.4 Pros and Cons

Wu et al. (2015) have reviewed the pros and cons of biosynthesis of iron oxide NPs (using various plants and microbes) in comparison to other synthetic methods (e.g. co-precipitation, microemulsion, electrochemical approach, thermal decomposition, sonolysis, aerosol/vapour methods, etc.). Phytosynthesis of iron oxide NPs is considered to be a greener (involving a lesser use of hazardous chemicals) and eco-friendly approach. Furthermore, the obtained products exhibit better biocompatibility than the counterparts produced by other methods. Phytosynthesis is executed under ambient atmospheric conditions and room temperature; however, the yield is low. The reaction period may extend from few minutes or hours to days. Furthermore, the precise tuning of size and shape of iron oxide NPs prepared via phytosynthesis is a challenge and needs greater delving.

9.3 Representative Endeavours

A number of recent reports testify the application of various plant parts like stem, leaves, fruits, flowers, roots and seeds as well as various phytocompounds for the preparation and stabilization of iron oxide NPs. Tracing the yesteryears, Shahwan et al. (2011) reported the fabrication of green tea extract-based iron NPs rich in iron oxide and oxyhydroxide, behaving as Fenton-like catalyst for the removal of cationic (methylene blue) and anionic (methyl orange) dyes. On parallel lines, Ahmmad et al. (2013) synthesized photocatalytic hematite nanoparticles (average size, 60 nm, and surface area 22.5m^2 g^{-1}) using *Camellia sinensis* leaf extract. On the other hand, superparamagnetic IO/Au NPs (~30 nm) were prepared using grape seed proanthocyanidin (GSP) extract at room temperature by Narayanan et al. (2012). Awwad and Salem (2012) reported single-step *carob*-leaf-based synthesis of monodispersed iron oxide NPs (4–8 nm) with crystalline structure.

Phumying et al. (2013) synthesized *aloe vera* leaf extract-based superparamagnetic Fe_3O_4 (6–30 nm), the saturation magnetization of which rose with increase in temperature and time. Huang et al. (2014) used polyphenols and caffeine-rich oolong tea extract for the synthesis of Fe-based (40–50 nm) NPs (zero-valent iron (α-Fe), maghemite (γ-Fe_2O_3), magnetite (Fe_3O_4) and iron hydroxides), which were tested for their capacity to degrade malachite green dye. *Dodonaea viscosa* leaf extract was used by Daniel et al. (2013) to prepare iron oxide NPs (~27 nm). The extract contained flavonoids, tannin and saponins that acted as the reducing and capping agent. The NPs were reported to exhibit antibacterial activity against a number of human pathogens viz. *Bacillus subtilis*, *Klebsiella pneumonia*, *Pseudomonas fluorescens* and *Staphylococcus aureus*. In another study, Venkateswarlu et al. (2013) reported the synthesis of iron oxide NPs using the extract of plantain peel. The nearly polydispersed NPs exhibited high saturation magnetization (15.8 emu g^{-1}), particle size less than 50 nm and surface area in the range of 11.31m^2 g^{-1}. Venkateswarlu et al. (2014a) also reported the synthesis of polycrystalline, ferromagnetic iron oxide NPs, using *Punica granatum* rind extract. The nanoparticles with surface-adhered plant-derived polyphenolics, high saturation magnetization (22.7 emu g^{-1}) and surface area of 10.88m^2 g^{-1} were used for the removal of Pb (II) ions from wastewater. Venkateswarlu et al. (2014b), in another study, documented the synthesis of ferromagnetic spherical iron oxide NPs (~20 nm) with inverse spinal face-centred cubic structure, using *Syzygium cumini* seed extract that acted as the reducing and capping agent. Sodium acetate present in the seed extract served as the electrostatic stabilizing agent. On the other hand, the stem extract of *Vitis vinifera* was used for the synthesis of polycrystalline iron oxide NPs (av. particle size <50 nm) with core-shell structure and high saturation magnetization (15.74 emu g^{-1}) (Venkateswarlu et al. 2015). Similarly, López-Téllez et al. (2013) synthesized iron oxide NPs (using an ethanol-treated orange peel) with rodlike shape for the remediation of chromium ion from wastewater. Cellulosic content present in orange peel served as the reducing and capping agent.

Balamurughan et al. (2014) used an extract of *Ocimum sanctum* for the synthesis of iron oxide NPs; SEM analysis was suggestive of aggregated appearance of the NPs with irregular spherical shape and rough surface. Makarov et al. (2014) reported the application of the extracts of *Hordeum vulgare* (pH 5.8) and *Rumex acetosa* (pH 3.7) for the fabrication of 30 nm- and 10–40 nm-sized iron oxide NPs, respectively. Organic acid such as oxalic and citric acid served as the reducing and capping agent. Kumar et al. (2014) used an extract of *Passiflora tripartita* var. *mollissima* fruit for the synthesis of magnetically recyclable, spherical iron oxide NPs (22.3 ± 3 nm), exhibiting high catalytic activity for the synthesis of 2-arylbenzimidazoles with excellent yields.

Herlekar and Siddhivinayak (2015) reported the microwave-assisted synthesis of evenly dispersed spherical iron oxide NPs using the extract of *Curcuma longa* (turmeric) leaves. These NPs were used to address orthophosphate contamination and chemical oxygen demand in domestic sewage. Esam (2015) synthesized iron oxide NPs (~45 nm) using Al-Abbas's (A.S.) Hund Fruit (*Citrus medica* var. s*arcodactylis*) extract. The antimicrobial application of the NPs was assessed against the bacteria present in Al-'alqami River. On the other hand, extract of *Hibiscus* leaf was used by Rath et al. (2015) to prepare superparamagnetic, monodispersed spherical iron oxide NPs (10–15 nm). Prasad (2016) reported the synthesis of crystalline iron oxide NPs (~30 nm) using *Mansoa alliacea* (garlic vine) leaf extract abundant with polyphenol, flavonoids and other antioxidants. Niraimathee et al. (2016) resorted to *Mimosa pudica* extract for the synthesis of spherical iron oxide NPs (av. size = 67 nm). The non-protein alkaloid, mimosine (β-3-hydroxy-4 pyridone amino acid, present in the root extract), was propounded as the major active agent, responsible for reducing ferrous sulphate into iron oxide NPs. Groiss et al. (2016) used an extract of *Cynometra ramiflora* leaves for the synthesis of crystalline iron oxide NPs with surface functional groups associated with the phytochemicals. They showed antibacterial activity against *E. coli* and *S. epidermidis*, while the attribute of Fenton-like catalyst was established using Rhodamine B dye.

Thakur and Karak (2014) resorted to banana-peel-ash aqueous extract as the base source and *Colocasia esculenta* leaves' aqueous extract as the reducing agent for fabrication of superparamagnetic iron oxide NPs decorated with reduced graphene oxide (RGO). Iron oxide/RGO nanocomposite could effectively remove Pb^{2+} and Cd^{2+} within 10 min, whereas tetrabromobisphenol A within 30 min, following a pseudo-second-order adsorption kinetics.

Thus, one can easily comprehend that iron oxide NPs have been prepared using a wide varieties of plant extracts. Let us now delve into some of the documented applications of the phytogenerated iron oxide NPs.

9.4 Spectrum of Applications

A wide array of applications of iron oxide NPs has been documented in diverse realms over the years. The following section mirrors some of the novel applications of iron oxide NPs, prepared via phytosynthetic approach.

9.4.1 Biomedical Applications

The surmounting issue of antibiotic resistance has dictated researchers to explore alternative antimicrobial agents. Over the years, various nanomaterials including iron oxide NPs have been investigated for their antimicrobial potency. A number of studies vouch for the successful biomedical applications of iron oxide NPs (as testified by recent reports cited in subsequent sections). However, establishing the biocompatibility of iron oxide NPs is a prerequisite for their application in anticancer therapy or as antimicrobial agents. Investigation of interactions of NPs with the possible 'interactomes' of the prokaryotic and eukaryotic cells has been a major focus of recent research. To illustrate these aspects, Khalil et al. (2017) executed an elaborate study on iron oxide NPs prepared by using the aqueous extract of *Sageretia thea*. Five human pathogenic bacterial strains exhibited differential susceptibility towards the iron oxide NPs, *Pseudomonas aeruginosa* (MIC, 7.4 μg mL^{-1}) being the most susceptible. The compatibility at the bio-interface for prospective biomedical applications was attested by high IC_{50} value (>200 μg mL^{-1}) for human RBCs and macrophages. It is pertinent to note that 17.2 and 16.75 μg mL^{-1} were the IC_{50} values for the promastigote and amastigote cultures of *Leishmania tropica* (suggestive of plausible use of the iron oxide NPs in anti-leishmanial therapy), while the assessment of cytotoxic potential using brine shrimps (*Artemia salina*, used as standard to screen cytotoxic compounds) revealed an IC_{50} value of 16.46 μg mL^{-1}. Internalization of iron oxide NPs via receptor-mediated endocytosis and subsequent Fe^{2+} dissolution leading to interference with the stability of the various proteins, entry into mitochondria as well as genotoxicity due to ROS generation are some of the proposed routes of toxicity of iron oxide NPs. The authors further established the protein kinase (PK) (a key enzyme, targeted in cancer therapy) inhibitory potential of iron oxide NPs using *Streptomyces* 85E strain as the test organism where the enzyme plays a prime role in hyphae formation. In the absence of iron oxide NPs, the growth factors are phosphorylated (leading to their activation) by PK in response to growth stimuli. On the other hand, interference of iron oxide NPs limits the potential of PK to initiate the domino effect of the signalling cascade, thereby resulting in the inhibition of division. Thus, these preliminary investigations are suggestive of the indispensable requisite for detailed- and long-term in vitro and in vivo investigations prior to commercialization of phytogenerated iron oxide NPs. Having said that, let us peruse some of the recent reports on the biomedical applications of iron oxide NPs.

9.4.1.1 Antagonist to Microbes and Disease Vectors

In an approach to investigate the prospects of food-processing waste for nanobiotechnological application, Patra and Baek (2017) used silky hairs of corn (*Zea mays*) and outer leaves of Chinese cabbage (*Brassica rapa* L. subsp. *pekinensis*)

under photo-catalyzed condition for fabricating superparamagnetic iron oxide NPs, with crystallite size of 84.81 and 48.91 nm, respectively. Apart from exhibiting antioxidant property, iron oxide NPs showed synergistic antibacterial action (on mixing with kanamycin and rifampicin) against pathogenic foodborne bacteria as well as anti-candidal activity (on mixing with amphotericin b) against five different *Candida* species. In a similar study, antibacterial activity of iron oxide NPs, fabricated using *Punica granatum* peel extract, had been reported against *Pseudomonas aeruginosa* (Irshad et al. 2017). The nonhaemolytic activity of the iron oxide NPs was projected as an index for establishing the biocompatibility of the iron oxide NPs. On the other hand, Fe_3O_4-Ag core-shell NPs, synthesized using *Vitis vinifera* stem extract as the green solvent, reducing and capping agent, were established as a potent antibacterial agent against gram-positive and gram-negative pathogens (Venkateswarlu et al. 2015). Antimicrobial activity of spherical iron oxide NPs (20–90 nm) prepared by ultrasound-assisted *Coriandrum sativum* leaf extract has been evaluated against *Micrococcus luteus*, *Staphylococcus aureus* and *Aspergillus niger* (Sathya et al. 2017). Researchers have also resorted to various marine plants for preparation of iron oxide NPs. El-Kassas and Ghobrial (2017) used the aqueous extract of *Halophila stipulacea*, rich in protein and polyphenols, to prepare iron oxide NPs exhibiting antagonistic action towards cyanobacteria, *Oscillatoria simplicissima* (known for the production of neurotoxins and its detrimental effects on various aquatic species). Mixed phase (α-Fe_2O_3 and γ-Fe_2O_3) spherical IO-NPs, prepared using the leaf extract of *Platanus orientalis*, were found to exhibit antifungal activity against *Aspergillus niger* and *Mucor piriformis*, the effect being more pronounced towards the latter (Devi et al. 2018).

On the other hand, in an effort to develop effective strategy to control filariasis vectors, Murugan et al. (2018) used *Ficus natalensis* aqueous extract and chemical nanosynthesis to prepare Fe_2O_3 NPs that demonstrated an LC_{50} ranging between 4.5 and 22.1 ppm against I instar larval and pupal stage of *Culex quinquefasciatus*.

9.4.1.2 Diagnostic and Curative (Anticancer) Properties

In vitro cytotoxicity of NPs prepared through green strategy (plant-mediated approach) depends on the concentration, exposure time and type of cells used for assessment (Saranya et al. 2017). Application of iron oxide NPs has been proposed for cancer therapy (Mohanasundaram et al. 2017). Iron oxide NPs, prepared using hydroethanolic leaf extract of *Annona squamosa*, were found to exhibit significant cytotoxicity on HepG2 and melanoma A375 cell lines in contrast to complete compatibility with normal liver cell line. Cubic-shaped iron oxide NPs (Fe_3O_4, 18 ± 4 nm) based on the seaweed, *Sargassum muticum*, exhibited anticancer activity (test duration, 72 h) against HepG2, MCF-7, HeLa and Jurkat cells, the corresponding IC_{50} values being 23.83 ± 1.1 μg mL^{-1}, 18.75 ± 2.1 μg mL^{-1}, 12.5 ± 1.7 μg mL^{-1} and 6.4 ± 2.3 μg mL^{-1} (Namvar et al. 2014). The reducing and capping potencies of aqueous extracts of *Vanilla planifolia* and *Cinnamomum verum* were exploited to

prepare polyphenol-coated magnetic NPs with core-shell Fe_3O_4-γFe_2O_3 structure, av. size 10–14 nm, and considerably high saturation magnetization values (70.84 emu g^{-1} and 59.45 emu g^{-1} for *C. verum* and *V. planifolia* mediated samples, respectively) (Ramirez-Nuñez et al. 2018). The plausibility of NPs application in magnetic hyperthermia was vouched by their efficacy to induce in vitro death of BV2 microglial cells post 30 min at a target temperature of 46 °C. However, it is appropriate to mention here that a number of factors have posed major hurdles in clinical trials of the biogenic nanomaterials against cancer. The issues include the selection of dosage and route of administration, biodegradability and biocompatibility, uptake, retention and clearance as well as the combinatorial approach with FDA-approved anticancer drugs (Barabadi et al. 2017).

On the other hand, in an interesting study to harness the biomedical utility of 'green' iron oxide NPs, ginger (*Zingiber officinale*) rhizome extract was effectively exploited as a capping agent for self-organizing Ag and iron oxide NPs in a single-step synthesis protocol, yielding highly ordered hierarchical microstructure, dictated by the ginger polysaccharides and water molecules (Ivashchenko et al. 2017). Bactericidal and fungicidal activity as well as magnetic resonance imaging (MRI) T2 contrasting and fluorescence attributes established the multimodality of the MAg NPs. It is relevant to mention that relaxivity values (R1 and R2) are used to assess a potential MRI contrast agent. The effect of MAg was evident only on the proton T2 relaxation, the results being dictated by the Fe concentration and the kind of dispersive medium. A decrease in the R2 relaxivity was documented from the sample MAg (Ag 10%) to MAg (Ag 33%) (Table 9.2).

On the other hand, as shown in Fig. 9.2a, the fluorescence 3D image revealed the accumulation of NPs in the surrounding areas of yeast cells. The experiment was conducted without the fluorescence dye (concanavalin A). Even without the membrane contour, the cells could be visualized. The observations suggested that the MAg could be employed in the studies of cells/NP interactions without the use of extra fluorescent agent adhered to the surface of the NPs.

Table 9.2 The relaxivity data of MAg as a T_2 contrast agent

Ag content in the sample, Mass %	Dispersive medium	Relaxivity data		
		R_1 mM^{-1} S^{-1}	R_1 mM^{-1} S^{-1}	R_2/R_1
10	Water	0.33 ± 0.02	25.6 ± 0.1.3	77.52
10	BSA (1%)	0.17 ±. 0.05	37.3 ± 0.2.4	219.59
22	Water	0.36 ± 0.0.02	20 ± 2	56.08
22	BSA (1%)	0.11 ± 0.0.03	12.2 ± 0.0.7	110.55
33	Water	0.29 ± 0.0.02	6.7 ± 0.0.4	23.14
33	BSA (1%)	0.16 ± 0.0.02	7.6 ±. 0.6	47.25

Reproduced from Ivashchenko et al. (2017)

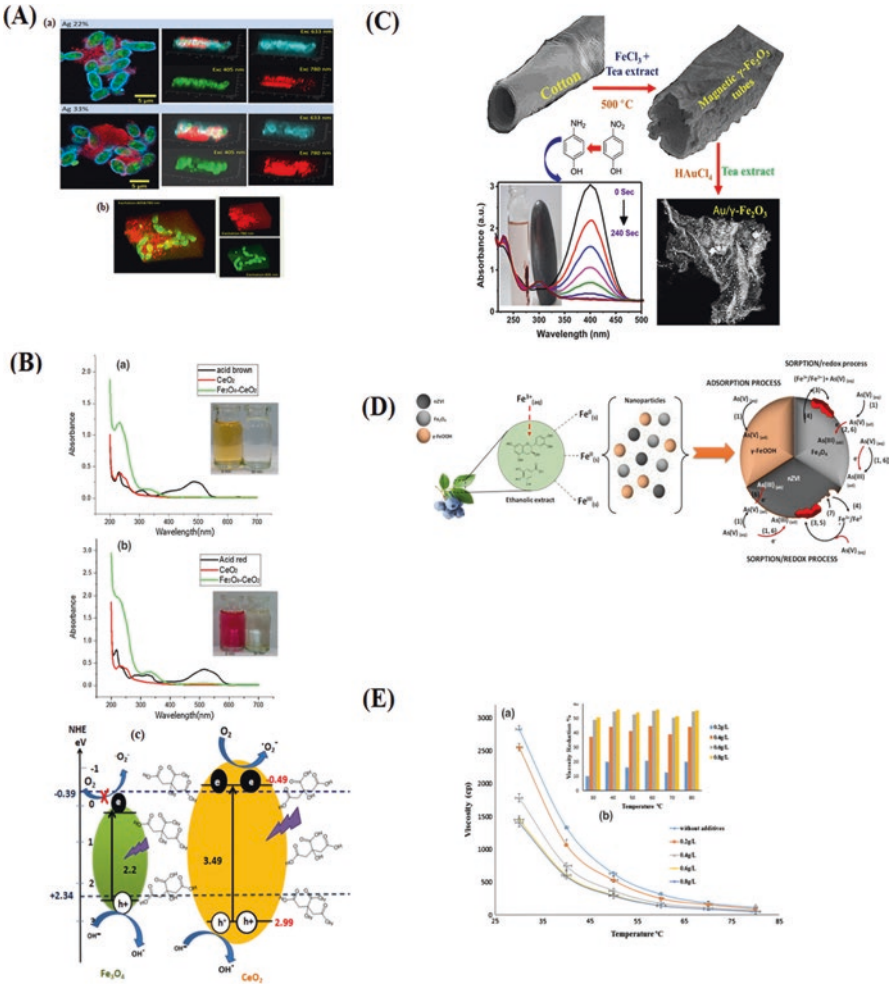

Fig. 9.2 (**a**) Fluorescence 3D images of yeast cells incubated with MAg (100 μg/mL) for 1 h (*a*) with and (*b*) without fluorescence dye. (Reproduced from Ivashchenko et al. 2017.) (**b**) Plot for change in the absorption spectrum of (*a*) acid brown and (*b*) acid red by Fe_3O_4–CeO_2. A model for the photocatalytic mechanism of the Fe_3O_4.CeO_2 nanocomposite. (Reproduced from Moradi et al. 2018.) (**c**) Metal (Au, Pd, Ag)-deposited magnetic γ-Fe_2O_3 tubular morphology was synthesized using cotton fibre as a sacrificial template. The developed material shows promising catalytic activity for the reduction of 4-nitrophenol to 4-aminophenol with a very good recyclability for the reuse of the catalyst. (Reproduced from Purbia and Paria 2018.) (**d**) Schematic representation of the possible mechanisms of As (V) removal and structural changes in lepidocrocite (γ-FeOOH), magnetite (FeO) and nZVI. Depending on the iron nanoparticles, As (V) can be removed by adsorption (*1*), absorption (*2*), precipitation (*3*), dissolution (*4*), co-precipitation (*5*) and reduction (*6*). The structure of nZVI is determined by dissolution or passivation (*4* and *7*). (Reproduced from Manquián-Cerda et al. 2017.) (**e**) (*a*) Oil viscosity vs. temperature for heavy oil before and after adding iron oxide NRs with different wt%. (*b*) An inset column chart shows viscosity reduction % at each temperature and additives wt%. (Reproduced from Al-Ruqeishi et al. 2016)

9.4.2 Dye-Adsorption/Degradation

Beheshtkhoo et al. (2018) have reported 81% dye-decolorization efficiency of iron oxide NPs (6.5–14.9 nm), prepared using the aqueous leaf extract of *Daphne mezereum*. Tharunya et al. (2017) employed ethanolic extract of *Ficus carica* fruit for a rapid, single-step reduction of ferrous sulphate solution to prepare superparamagnetic iron oxide NPs for degradation of dyes. On the other hand, monodispersed, superparamagnetic Fe_3O_4-CeO_2 nanocomposites were prepared basing on a hydrothermal method coupled to a greener protocol involving lemon extract (Moradi et al. 2018). The efficient and rapid degradation of two azo dyes under ultraviolet light irradiation established their prospective photocatalytic application (Fig. 9.2b). Similarly, Carvalho and Carvalho (2017) reported the rapid and complete decolourization of different dyes using carbon-rich catalysts based on iron (II)/(III) oxides and oxyhydroxides composites (over silica), prepared with *Camellia sinensis* extract.

9.4.3 Catalysis

Recently, Shahriary et al. (2018) have exploited the extract of *Stachys lavandulifolia* ("Chaye-e-Kohi" a native of Iran) for fabrication of a hybrid magnetic nanocomposite, with antibacterial efficacy, documented against *E. coli* and *S. aureus*. The Fe_3O_4 NPs with carbonyl and phenolic hydroxyl surface functionality, conferred by the biomolecules of the herbal tea extract, acted as the edifice for the in situ generation of silver NPs. The recyclable nanocomposite exhibited high catalytic activity for 4-nitrophenol reduction at ambient temperature. In yet another interesting study, natural cotton fibres were used as sacrificial template for the fabrication of Au, Ag and Pd nanoparticle-decorated hierarchical maghemite tubes, using green tea extract (Purbia and Paria 2018). Effective catalytic potency of the magnetically recyclable nanocatalyst was demonstrated for the hydrogenation reaction of 4-nitrophenol to aminophenol conversion (Fig. 9.2c). Fe_3O_4 nanocatalysts were prepared by Shojaee and Mahdavi Shahri (2018) using an aqueous extract of *Camellia sinensis*. The magnetically recyclable catalysts were efficiently used for the one-pot synthesis of 2-(4-chlorophenyl)-1H-benzo[*d*]imidazole that exhibited dose-dependent in vitro toxicity on MOLT-4 cells. The study vouched for the potential of iron oxide NPs, prepared by greener route for preparation of biomedically relevant therapeutic materials.

9.4.4 Eco-Hazard Mitigation/Metal-Ion Adsorption

Recalcitrant chlorobenzenes are listed as priority pollutants by the US Environmental Protection Agency (USEPA). In this context, Kuang et al. (2013) reported the synthesis of zero-valent iron (α-Fe), maghemite (γ-Fe_2O_3), magnetite (Fe_3O_4) and iron

hydroxides using extracts of green tea, oolong tea and black tea. These irregular spherical NPs (with basic size: 20–40 nm and surface area of 5.82m^2 g^{-1}) could mediate Fenton-like oxidation of mono-chlorobenzene (MCB) owing to their high surface and reactivity, complemented by low leaching of Fe^{2+}. The correspondence between oxidative degradation efficacy and the associated COD removal was suggestive of the partial mineralization of MCB to carbon dioxide and water. On the other hand, Hassan et al. (2018) have demonstrated the application of iron oxide NPs, prepared using pomegranate peel extract, for adsorption of pyrene and benzo (α) pyrene. Following a pseudo-second-order mechanism of adsorption, the NPs exhibited more than 98% removal of the polycyclic aromatic hydrocarbons (PAH) from artificially contaminated water in a semi-pilot plant.

Various reports evince the use of iron oxide NPs for adsorption of metal ions. In an endeavour to develop an efficient adsorbent to remove Ni (II) ions, superparamagnetic iron oxide NPs were prepared using *Lantana camara* extract as the stabilizer and ammonia solution as the precipitating agent for Fe^{2+} and Fe^{3+} salts in water (Nithya et al. 2018). These NPs exhibited remarkably high adsorption capacity of 227.2 mg g^{-1} at a pH of 6.0 and adsorbent dose of 0.05 g. In another study, Lunge et al. (2014) reported the preparation of iron oxide NPs using an extract of tea waste at room temperature for removal of As (III) and As (V). It was observed that the maximum adsorption of As (III) and As (V) was 188.7 mg g^{-1} and 153.8 mg g^{-1} at neutral pH, respectively. Extract of leaves and shoots of blueberry (*Vaccinium corymbosum*) was used for the preparation of diverse NPs, varying in forms and associated structures, including lepidocrocite and magnetite (Manquián-Cerda et al. 2017). These were projected as an effective material for arsenic (As) (V) remediation (Fig. 9.2d). Iron oxide NPs, prepared using the extract of tangerine peels, were employed for the remediation of cadmium ions from waste water (Ehrampoush et al. 2015). Similarly, IO-NPs, synthesized using the extract of *Excoecaria cochinchinensis* leaves and subsequently modified by low-temperature calcination, were effectively used to adsorb ~98.50% of Cd (II) (10 mg L^{-1}) under optimized parameters (based on Box Behnken Design) of pH, absorbent dosage, temperature and ionic strength conditions as 8.07, 2.5 g L^{-1}, 45 °C and 0.07 mol L^{-1}, respectively (Lin et al. 2018). In an interesting study, Rao et al. (2013) obtained surface modification of *Yarrowia lipolytica* (NCIM 3589 and NCIM 3590) cells with phytoinspired Fe^0/Fe_3O_4 NPs in an effort to remove hexavalent chromium ions. The reported nanocomposite displayed higher values of Langmuir and Scatchard coefficients than untreated cells, thus suggesting that the former was a better agent for mitigating Cr (VI) toxicity.

9.4.5 Heavy-Oil Viscosity Treatment

A reduction in dynamic viscosity of crude oil results in direct microwave irradiation. On impregnation of heavy oil with phytosynthesized iron oxide NRs (Al-Ruqeishi et al. 2016), the viscosity reduction rate was enhanced. Addition of 0.2 g of iron oxide NRs to 1 L of heavy oil led to a reduction of viscosity by 10% at

30 °C. On the other hand, a further augmentation (up to 38% and 49%) in the viscosity reduction was noted for 0.4 and 0.6 g L^{-1} additives (0.8 g L^{-1} being the oil's additive saturation point) (Fig. 9.2e). Experts have forwarded the 'green' iron oxide NRs as befitting candidate for heavy crude oil cracking in the perspective of small size, distribution and thermal conversion.

9.4.6 Augmenting the Agricultural Output

Investigating the effect of nanomaterials on agricultural domain has been an interesting proposition. In this context, Sebastian et al. (2017) have recommended application of iron oxide NPs, synthesized using caffeic acid as a potential ameliorant, as a solution to Ca-induced Fe deficiency in *Oryza sativa* (rice). Bioproductivity, photosynthetic electron transport, antioxidant enzyme activity and iron accumulation under calcium stress were augmented. In an endeavour to develop green materials for environmental remediation, Sebastian et al. (2018) reported that iron oxide NPs with surface-fabricated phenolics from coconut husk could efficiently adsorb Ca and Cd. However, the interesting attribute of the study was the augmented iron accumulation in rice plants as well as tolerance towards calcium and cadmium stress. Increase of biomass and chlorophyll content attested the plant-growth-accelerating action of the iron oxide NPs.

9.5 Conclusion

Although a plethora of plants have been explored for fabrication of iron oxide NPs, it is fascinating to observe the real-time genesis of the exotic iron oxide nanostructures reported in a number of studies. Optimization of the process parameters to arrest the growth of iron oxide NRs at a particular stage could be another focus area. Use of advanced analytical and computational tools would complement our understanding on the possible evolution and structural modulations of the iron oxide NPs, mediated by the phytocompounds. Despite the fact that phytosynthesis is considered as a benign approach for preparing iron oxide NPs, it is crucial to note that nanomaterials prepared through green strategy may not be 'green' per se with respect to their action at the biological interface. The shape-size-surface chemistry-concentration accord dictates the bio-nano-interfacial outcome. Compilation of toxicity profile of the iron oxide NPs is a must prior to their commercial applications. Probing the actions at the in vitro and in vivo levels is indispensable. The experimental biocompatibility assessments may be complemented (not substituted) by computational techniques like quantitative structure-activity-relationship (QSAR) method. Execution of a 'cradle-to-grave' analysis would assist in realizing the actual application potential of iron oxide NPs. Nevertheless, the portal to several prospective applications of phytogenerated iron oxide NPs has just been opened.

References

Ahmmad B, Leonard K, Islam MS, Kurawaki J, Muruganandham M, Ohkubo T, Kuroda Y (2013) Green synthesis of mesoporous hematite (a-Fe2O3) nanoparticles and their photocatalytic activity. Adv Powder Technol 24:160–167

Ali A, Zafar H, Zia M, UL Haq I, Phull AR, Ali JS, Hussain A (2016) Synthesis, characterization, applications, and challenges of iron oxide nanoparticles. Nanotechnol Sci Appl 9:49–67

Al-Ruqeishi MS, Mohiuddin T, Al-Saadi LK (2016) Green synthesis of iron oxide nanorods from deciduous Omani mango tree leaves for heavy oil viscosity treatment. Arab J Chem. https://doi.org/10.1016/j.arabjc.2016.04.003

Awwad AM, Salem NM (2012) A green and facile approach for synthesis of magnetite nanoparticles. Nanosci Nanotechnol 2:208–213

Balamurughan MG, Mohanraj S, Kodhaiyolii S, Pugalenthi V (2014) *Ocimum sanctum* leaf extract mediated green synthesis of iron oxide nanoparticles: spectroscopic and microscopic studies. J Chem Pharma Sci Special Issue 4:201–204

Barabadi H, Ovais M, Shinwari ZK, Saravanan M (2017) Anti-cancer green bionanomaterials: present status and future prospects. Green Chem Lett Rev 10:285–314

Barreto JC, Trevisan MT, Hull WE, Erben G, Brito ESD, Pfundstein B, Würtele G, Spiegelhalder B, Owen RW (2008) Characterization and quantitation of polyphenolic compounds in bark, kernel, leaves, and peel of mango (*Mangifera indica* L). J Agric Food Chem 56:5599–5610

Barua S, Konwarh R, Mandal M, Gopalakrishnan R, Kumar D, Karak N (2013) Biomimetically prepared antibacterial, free radical scavenging poly(ethylene glycol) supported silver nanoparticles as *Aedes albopictus* larvicide. Adv Sci Eng Med 5:291–298

Beheshtkhoo N, Kouhbanani MAJ, Savardashtaki A, Amani AM, Taghizadeh S (2018) Green synthesis of iron oxide nanoparticles by aqueous leaf extract of *Daphne mezereum* as a novel dye removing material. Appl Phys A Mater Sci Process 124:363

Can HK, Kavlak S, ParviziKhosroshahi S, Güner A (2018) Preparation, characterization and dynamical mechanical properties of dextran-coated iron oxide nanoparticles (DIO-NPs). Artif Cells Nanomed Biotechnol 46:421–431

Carvalho SS, Carvalho NM (2017) Dye degradation by green heterogeneous Fenton catalysts prepared in presence of *Camellia sinensis*. J Environ Manag 187:82–88

Daniel SK, Vinothini G, Subramanian N, Nehru K, Sivakumar M (2013) Biosynthesis of Cu, ZVI, and Ag nanoparticles using *Dodonaea viscosa* extract for antibacterial activity against human pathogens. J Nanopart Res 15:1319

Devi HS, Boda MA, Shah MA, Parveen S, Wani AH (2018) Green synthesis of iron oxide nanoparticles using *Platanus orientalis* leaf extract for antifungal activity. Green Process Synth 1–8. https://doi.org/10.1515/gps-2017–0145

Dinali R, Ebrahiminezhad A, Manley-Harris M, Ghasemi Y, Berenjian A (2017) Iron oxide nanoparticles in modern microbiology and biotechnology. Crit Rev Microbiol 43:493–507

Ehrampoush MH, Miria M, Salmani MH, Mahvi AH (2015) Cadmium removal from aqueous solution by green synthesis iron oxide nanoparticles with tangerine peels extract. J Environ Health Sci Eng 13:84

El-Kassas HY, Ghobrial MG (2017) Biosynthesis of metal nanoparticles using three marine plant species: anti-algal efficiencies against *Oscillatoria simplicissima*. Environ Sci Pollut Res 24(8):7837–7849

Esam JAK (2015) Green synthesis of magnetite iron oxide nanoparticles by using Al-Abbas's (AS) hund fruit (*Citrus medica*) var. Sarcodactylis Swingle extract and used in Al-'alqami river water treatment. J Nat Sci Res 5:125–135

Feng Q, Liu Y, Huang J, Chen K, Huang J, Xiao K (2018) Uptake, distribution, clearance, and toxicity of iron oxide nanoparticles with different sizes and coatings. Sci Rep 8:2082

Gan L, Lu Z, Cao D, Chen Z (2018) Effects of cetyltrimethylammonium bromide on the morphology of green synthesized Fe_3O_4 nanoparticles used to remove phosphate. Mater Sci Eng 82:41–45

Groiss S, Selvaraj R, Thivaharan V, Vinayagam R (2016) Structural characterization, antibacterial and catalytic effect of iron oxide nanoparticles synthesised using the leaf extract of *Cynometra ramiflora*. J Mol Struct 1128:572–578

Hassan SS, Abdel-Shafy HI, Mansour MS (2018) Removal of pyrene and benzo (a) pyrene micropollutant from water via adsorption by green synthesized iron oxide nanoparticles. Adv Nat Sci Nanosci Nanotech 9:015006

Herlekar M, Siddhivinayak B (2015) Optimization of microwave assisted green synthesis protocol for iron oxide nanoparticles and its application for simultaneous removal of multiple pollutants from domestic sewage. Int J Adv Res 3:331–345

Herrera-Becerra R, Zorrilla C, Rius JL, Ascencio JA (2008) Electron microscopy characterization of biosynthesize iron oxide nanoparticles. Appl Phy A 91:241–246

Huang L, Weng X, Chen Z, Megharaj M, Naidu R (2014) Synthesis of iron-based nanoparticles using oolong tea extract for the degradation of malachite green. Spectrochim Acta A Mol Biomol Spectrosc 117:801–804

Husen A (2017) Gold Nanoparticles from plant system: synthesis, characterization and their application. In: Ghorbanpour M, Manika K, Varma A (eds) Nanoscience and plant–soil systems, vol 48. Springer, Cham, pp 455–479

Husen A, Siddiqi KS (2014) Phytosynthesis of nanoparticles: concept, controversy and application. Nanoscale Res Lett 9:229

Irshad R, Tahira K, Li B, Ahmada A, Siddiquia AR, Nazir S (2017) Antibacterial activity of biochemically capped iron oxide nanoparticles: a view towards green chemistry. J Photochem Photobio B 170:241–246

Ivashchenko O, Gapiński J, Peplińska B, Przysiecka Ł, Zalewski T, Nowaczyk G, Jarek M, Marcinkowska-Gapińska A, Jurga S (2017) Self-organizing silver and ultrasmall iron oxide nanoparticles prepared with ginger rhizome extract: characterization, biomedical potential and microstructure analysis of hydrocolloids. Mater Des 133:307–324

Izadiyan Z, Shameli K, Miyake M, Hara H, Mohamad SEB, Kalantari K, Taib SHM, Rasouli E (2018) Cytotoxicity assay of plant-mediated synthesized iron oxide nanoparticles using *Juglans regia* green husk extract. Arabian J Chem. https://doi.org/10.1016/j.arabjc.2018.02.019

Jun YW, Seo JW, Cheon J (2008) Nanoscaling laws of magnetic nanoparticles and their applicabilities in biomedical sciences. Acc Chem Res 41:179–189

Khalil AT, Ovais M, Ullah I, Ali M, Shinwari ZK, Maaza M (2017) Biosynthesis of iron oxide (Fe_2O_3) nanoparticles via aqueous extracts of *Sageretia thea* (Osbeck) and their pharmacognostic properties. Green Chem Lett Rev 10:186–201

Konwarh R, Karak N, Rai SK, Mukherjee AK (2009) Polymer-assisted iron oxide magnetic nanoparticle immobilized keratinase. Nanotechnology 20:225107

Konwarh R, Kalita D, Mahanta C, Mandal M, Karak N (2010) Magnetically recyclable, antimicrobial, and catalytically enhanced polymer-assisted green nanosystem-immobilized *Aspergillus niger* amyloglucosidase. Appl Microbiol Biotechnol 87:1983–1992

Konwarh R, Pramanik S, Devi KSP, Saikia N, Boruah R, Maiti TK, Deka RC, Karak N (2012) Lycopene coupled 'trifoliate' polyaniline nanofibers as multi-functional biomaterial. J Mater Chem 22:15062–15070

Konwarh R, Shail M, Medhi T, Mandal M, Karak N (2014) Sonication assisted assemblage of exotic polymer supported nanostructured bio-hybrid system and prospective application. Ultrason Sonochem 21:634–642

Kuang Y, Wang Q, Chen Z, Megharaj M, Naidu R (2013) Heterogeneous Fenton-like oxidation of monochlorobenzene using green synthesis of iron nanoparticles. J Colloid Interface Sci 410:67–73

Kumar KM, Mandal BK, Kumar KS, Reddy PS, Sreedhar B (2013) Biobased green method to synthesise palladium and iron nanoparticles using *Terminalia chebula* aqueous extract. Spectrochim Acta A Mol Biomol Spectrosc 102:128–133

Kumar B, Smita K, Cumbal L, Debut A (2014) Biogenic synthesis of iron oxide nanoparticles for 2-arylbenzimidazole fabrication. J Saudi Chem Soc 18:364–369

Kumar JP, Konwarh R, Kumar M, Gangrade A, Mandal BB (2017) Potential nanomedicine applications of multifunctional carbon nanoparticles developed using green technology. ACS Sustain Chem Eng 6:1235–1245

Latha N, Gowri M (2014) Bio synthesis and characterisation of Fe3O4 nanoparticles using *caricaya papaya* leaves extract. Syn Int J Sci Res 3:1551–1556

Lin J, Su B, Sun M, Bo C, Zuliang C (2018) Biosynthesized iron oxide nanoparticles used for optimized removal of cadmium with response surface methodology. Sci Total Environ 627:314–321

López-Téllez G, Balderas-Hernández P, Barrera-Díaz CE, Vilchis-Nestor AR, Roa-Morales G, Bilyeu B (2013) Green method to form iron oxide nanorods in orange peels for chromium (VI) reduction. J Nanosci Nanotechnol 13:2354–2361

Lunge S, Singh S, Sinha A (2014) Magnetic iron oxide (Fe_3O_4) nanoparticles from tea waste for arsenic removal. J Magn Magn Mater 356:21–31

Makarov VV, Makarova SS, Love AJ, Sinitsyna OV, Dudnik AO, Yaminsky IV, Taliansky ME, Kalinina NO (2014) Biosynthesis of stable iron oxide nanoparticles in aqueous extracts of *Hordeum vulgare* and *Rumex acetosa* plants. Langmuir 30:5982–5988

Manquián-Cerda K, Cruces E, Angélica RM, Reyes C, Arancibia-Miranda N (2017) Preparation of nanoscale iron (oxide, oxyhydroxides and zero-valent) particles derived from blueberries: reactivity, characterization and removal mechanism of arsenate. Ecotoxicol Environ Saf 145:69–77

Mirza AU, Kareem A, Nami SAA, Khan MS, Rehman S, Bhat SA, Mohammad A, Nishat N (2018) Biogenic synthesis of iron oxide nanoparticles using Agrewia optiva and Prunus persica phyto species: characterization, antibacterial and antioxidant activity. J Photochem Photobiol B 185:262–274

Mobasser S, Firoozi AA (2016) Review of nanotechnology applications in science and engineering. J Civil Eng Urban 6:84–93

Mohanasundaram S, Hemalatha S, Vanitha V, Bharathi NP, Jayalakshmi M, Pushpabharathi N (2017) Deciphering the cytotoxic activity of *Annona squamosa* iron oxide nanoparticles against selective cancer cell line. Int J Res Pharm Sci 8(2):259–263

Moradi B, Nabiyouni G, Ghanbari D (2018) Rapid photo-degradation of toxic dye pollutants: green synthesis of mono-disperse Fe_3O_4–CeO_2 nanocomposites in the presence of lemon extract. J Mater Sci Mater Electron 29(13):11065–11080

Murugan K, Dinesh D, Nataraj D, Subramaniam J, Amuthavalli P, Madhavan J, Rajasekar A, Rajan M, Thiruppathi KP, Kumar S, Higuchi A (2018) Iron and iron oxide nanoparticles are highly toxic to *Culex quinquefasciatus* with little non-target effects on larvivorous fishes. Environ Sci Pollut Res 25:10504–10514

Namvar F, Rahman HS, Mohamad R, Baharara J, Mahdavi M, Amini E, Chartrand MS, Yeap SK (2014) Cytotoxic effect of magnetic iron oxide nanoparticles synthesized via seaweed aqueous extract. Int J Nanomedicine 9:2479

Narayanan SBN, Sathy U, Mony M, Koyakutty S, Nair V, Menon D (2012) Biocompatible magnetite/gold nano hybrid contrast agents via green chemistry for MRI and CT bioimaging. ACS Appl Mater Interfaces 4:251–260

Neamtu M, Nadejde C, Hodoroaba VD, Schneider RJ, Verestiuc L, Panne U (2018) Functionalized magnetic nanoparticles: synthesis, characterization, catalytic application and assessment of toxicity. Sci Rep 8:6278

Niraimathee VA, Subha V, Ravindran RE, Renganathan S (2016) Green synthesis of iron oxide nanoparticles from Mimosa pudica root extract. Int J Environ Sustain Dev 15:227–240

Nithya K, Sathish A, Kumar PS, Ramachandran T (2018) Fast kinetics and high adsorption capacity of green extract capped superparamagnetic iron oxide nanoparticles for the adsorption of Ni (II) ions. J Ind Eng Chem 59:230–241

Patra JK, Baek KH (2017) Green biosynthesis of magnetic iron oxide (Fe3O4) nanoparticles using the aqueous extracts of food processing wastes under photo-catalyzed condition and investigation of their antimicrobial and antioxidant activity. J Photochem Photobiol B 173:291–300

Phumying S, Labuayai S, Thomas C, Amornkitbamrung V, Swatsitang E, Maensiri S (2013) *Aloe vera* plant-extracted solution hydrothermal synthesis and magnetic properties of magnetite (Fe_3O_4) nanoparticles. Appl Phys A Mater Sci Process 111(4):1187–1193

Plachtová P, Medříková Z, Zbořil R, Tuček J, Varma RS, Maršálek B (2018) Iron and Iron oxide nanoparticles synthesized with green tea extract: differences in ecotoxicological profile and ability to degrade malachite green. ACS Sustain Chem Eng 6:8679–8687

Pramanik S, Konwarh R, Deka RC, Aidew L, Barua N, Buragohain AK, Mohanta D, Karak N (2013) Microwave-assisted poly (glycidyl methacrylate)-functionalized multiwall carbon nanotubes with a 'tendrillar' nanofibrous polyaniline wrapping and their interaction at bio-interface. Carbon 55:34–43

Prasad AS (2016) Iron oxide nanoparticles synthesized by controlled bio-precipitation using leaf extract of garlic vine (*Mansoa alliacea*). Mater Sci Semicond Process 53:79–83

Purbia R, Paria S (2018) Noble metals decorated hierarchical maghemite magnetic tubes as an efficient recyclable catalyst. J Colloid Interface Sci 511:463–473

Ramirez-Nuñez AL, Jimenez-Garcia LF, Goya GF, Sanz B, Santoyo-Salazar J (2018) In vitro magnetic hyperthermia using polyphenol-coated Fe_3O_4@γFe_2O_3 nanoparticles from *Cinnamomun verum* and *Vanilla planifolia*: the concert of green synthesis and therapeutic possibilities. Nanotechnology 29:074001

Rao A, Bankar A, Kumar AR, Gosavi S, Zinjarde S (2013) Removal of hexavalent chromium ions by Yarrowia lipolytica cells modified with phyto-inspired Fe 0/Fe_3O_4 nanoparticles. J Contam Hydrol 146:63–73

Rath KB, Singh A, Chandan S (2015) Biosynthesis of magnetic iron oxide nanoparticles using Hibiscus as a plant source. NanoTrends 17:1–9

Reardon PJ, Konwarh R, Knowles JC, Mandal BB (2017) Mimicking hierarchical complexity of the osteochondral interface using electrospun silk-bioactive glass composites. ACS Appl Mater Interfaces 9:8000–8013

Santoshi V, Shakila Banu A, Kurian GA (2015) Synthesis, characterization and biological evaluation of iron oxide nanoparticles prepared by *Desmodium gangeticum* root aqueous extract. Int J Pharm Pharm Sci 7(13):75–80

Saranya S, Vijayaranai K, Pavithra S, Raihana N, Kumanan K (2017) In vitro cytotoxicity of zinc oxide, iron oxide and copper nanopowders prepared by green synthesis. Toxicol Rep 4:427–430

Sathya K, Saravanathamizhan R, Baskar G (2017) Ultrasound assisted phytosynthesis of iron oxide nanoparticle. Ultrason Sonochem 39:446–451

Sebastian A, Nangia A, Prasad MNV (2017) Carbon-bound iron oxide nanoparticles prevent calcium-induced iron deficiency in *Oryza sativa* L. J AgricFood Chem 65:557–564

Sebastian A, Nangia A, Prasad MNV (2018) A green synthetic route to phenolics fabricated magnetite nanoparticles from coconut husk extract: implications to treat metal contaminated water and heavy metal stress in *Oryza sativa* L. J Clean Prod 174:355–366

Senthil M, Ramesh C (2012) Biogenic synthesis of Fe3O4 nanoparticle using Tridax procumbens leaf extract and its antibacterial activity on *Pseudomonas aeruginosa*. Dig J Nanomater Biostruct 7:1655–1661

Shah M, Fawcett D, Sharma S, Tripathy SK, Poinern GEJ (2015) Green synthesis of metallic nanoparticles via biological entities. Materials 8:7278–7308

Shahriary M, Veisi H, Hekmati M, Hemmati S (2018) In situ green synthesis of Ag nanoparticles on herbal tea extract (*Stachys lavandulifolia*)-modified magnetic iron oxide nanoparticles as antibacterial agent and their 4-nitrophenol catalytic reduction activity. Mater Sci Eng C 90:57–66

Shahwan T, Sirriah SA, Nairat M, Boyacı E, Eroğlu AE, Scott TB, Hallam KR (2011) Green synthesis of iron nanoparticles and their application as a Fenton-like catalyst for the degradation of aqueous cationic and anionic dyes. Chem Eng J 172:258–266

Shojaee S, Mahdavi Shahri M (2018) An efficient synthesis and cytotoxic activity of 2-(4-chlorophenyl)-1H–benzo [d] imidazole obtained using a magnetically recyclable Fe_3O_4 nanocatalyst-mediated white tea extract. Appl Organomet Chem 32:e3934

Siddiqi KS, Husen A (2017) Recent advances in plant-mediated engineered gold nanoparticles and their application in biological system. J Trace Elem Med Biol 40:10–23

Siddiqi KS, Rahman A, Tajuddin HA (2016) Biogenic fabrication of iron/iron oxide nanoparticles and their application. Nano Res Lett 11:498

Siddiqi KS, Husen A, Rao RAK (2018a) A review on biosynthesis of silver nanoparticles and their biocidal properties. J Nanobiotechnol 16:14

Siddiqi KS, Husen A, Sohrab SS, Osman M (2018b) Recent status of nanomaterials fabrication and their potential applications in neurological disease management. Nano Res Lett 13:231

Sravanthi M, Kumar DM, Ravichandra M, Vasu G, Hemalatha KPJ (2016) Green synthesis and characterization of iron oxide nanoparticles using *Wrightiatinctoria* leaf extract and their antibacterial studies. Int J Curr Res Aca Rev 4:30–44

Sudha K, Anitta S, Devi PM, Thejomayah G (2015) Biosynthesis of iron nanoparticle from green banana peel extract. IJSSIR 4(6):165–176

Thakur S, Karak N (2014) One-step approach to prepare magnetic iron oxide/reduced graphene oxide nanohybrid for efficient organic and inorganic pollutants removal. Mater Chem Phys 144:425–432

Thakur S, Karak N (2015) Alternative methods and nature-based reagents for the reduction of graphene oxide: a review. Carbon 94:224–242

Tharunya P, Subha V, Kirubanandan S, Sandhaya S, Renganathan S (2017) Green synthesis of superparamagnetic iron oxide nanoparticle from *Ficus carica* fruit extract, characterization studies and its application on dye degradation studies. Asian J Pharm Clin Res 10:125–128

Venkateswarlu S, Rao YS, Balaji T, Prathima B, Jyothi NVV (2013) Biogenic synthesis of Fe3O4 magnetic nanoparticles using plantain peel extract. Mater Lett 100:241–244

Venkateswarlu S, Kumar BN, Prathima B, SubbaRao Y, Jyothi NVV (2014a) A novel green synthesis of Fe3O4 magnetic nanorods using Punica granatum rind extract and its application for removal of Pb (II) from aqueous environment. Arab J Chem. https://doi.org/10.1016/j.arabjc.2014.09.006

Venkateswarlu S, Kumar BN, Prasad CH, Venkateswarlu P, Jyothi NVV (2014b) Bio-inspired green synthesis of Fe_3O_4 spherical magnetic nanoparticles using *Syzygium cumini* seed extract. Physica B Condens Matter 449:67–71

Venkateswarlu S, Kumar BN, Prathima B, Anitha K, Jyothi NVV (2015) A novel green synthesis of Fe_3O_4-Ag core shell recyclable nanoparticles using Vitis vinifera stem extract and its enhanced antibacterial performance. Physica B Condens Matter 457:30–35

Wu W, Wu Z, Yu T, Jiang C, Kim WS (2015) Recent progress on magnetic iron oxide nanoparticles: synthesis, surface functional strategies and biomedical applications. Sci Technol Adv Mater 16:023501